Current Research in Food Science 4 (2021) 53–62

Contents lists available at ScienceDirect

Current Research in Food Science

journal homepage: www.editorialmanager.com/crfs/

Complex coacervation of food grade antimicrobial lauric arginate with lambda carrageenan

Trivikram Nallamilli *, Markus Ketomaeki, Domenik Prozeller, Julian Mars, Svenja Morsbach, Markus Mezger, Thomas Vilgis

Max Planck Institute for Polymer Research, Ackermannweg 10, 55128, Mainz, Germany

ARTICLE INFO

Keywords:
Isothermal titration calorimetry
Small angle X ray scattering
Turbidity
Catanionic micelles
Foam
Zetapotential
Surfactant bilayers
Teubner-strey structure factor model

ABSTRACT

In this study, the complex coacervation mechanism of Lauric arginate ester (LAE) with λ-carrageenan was studied using turbidimetry, light scattering and electrophoresis. The complexes formed were found to have a bilayer-like structure using small angle X-ray scattering (SAXS) and cryo-TEM (transmission electron microscopy). It was observed that mixing LAE with Sodium dodecyl sulfate (SDS) could significantly reduce the interactions between mixed micelles and λ-carrageenan. The interactions between LAE/SDS and λ-carrageenan were found to be predominantly entropy driven. Mixed micelles of LAE/Tween 20 and LAE/SDS showed significantly less interactions with carrageenan compared to pure LAE micelles. Interfacial properties of complexes were measured using surface tension measurements. It was observed that pure LAE showed good foaming behavior and when mixed with increasing amounts of carrageenan the foaming capacity decreased. Reduction in foam volume was due to reduced availability of free LAE molecules for foam stabilization and due to hydrophilic nature of complexes.

1. Introduction

Lauric arginate ester (LAE) is an approved food grade cationic surfactant (E243) with strong anti-microbial properties. LAE is synthesized from Lauric acid, ethyl alcohol and basic amino acid L-arginine. LAE is easily metabolised by the human body into its constituent components (Dai et al., 2010). Unlike many toxic cationic surfactants like Cetyl-trimethyl ammoniumbromide (Lau et al., 2012) (CTAB). LAE is not toxic to humans. It is widely used as a preservative in many food products such as processed meats, milk products and fruit juices (Hu et al., 2020).

LAE when used in food products also interacts with other negatively charged molecules like proteins and polysaccharides (Ma et al., 2020). These electrostatic interactions lead to formation of complex coacervates. This eventually reduces the efficiency of LAE and thus increases the minimum inhibitory concentration (MIC) of the LAE in given food applications. Hence, there is a need to understand the basic interactions between LAE and other components in a food matrix and devise methods to reduce the coacervate formation and thus improve the efficiency of LAE.

Complex coacervation is a liquid-liquid phase separation that occurs between colloidal entities like proteins, biopolymers, surfactants or nanoparticles due to different interactions *viz.* electrostatic interactions (Kevelam et al., 1996), hydrogen bonding (Okuzaki and Osada 1994), hydrophobic interactions (Kayitmazer, 2017), entropy gain (De Kruif, Weinbreck et al., 2004) due to release of bound counter ions and structural reorganization water molecules. It leads to a polymer rich coacervate phase and solvent rich aqueous phase. Coacervation is a fundamental mechanism in many processes ranging from synthetic (Stewart et al., 2011) and bio-inspired adhesives (Waite et al., 2005), food texture modifiers (Wu et al., 2014), drug encapsulents (Saravanan and Rao 2010), emulsifiers (Jun-xia, Hai-yan et al., 2011) and foaming aids (Miquelim et al., 2010) in food and cosmetic products (Martins et al., 2014) etc.

Several studies in recent years have explored and reported complex coacervation between cationic surfactants and anionic polysaccharides (Covis et al., 2015). reported coacervation behavior of cocamidopropyl betaine and carrageenans. In this study authors reported the formation of complex coacervates between surfactant and carrageenan due to electrostatic interactions (Asker et al., 2008). reported on interactions of LAE with Pectin, where the interaction were found to be exothermic using Isothermal Titration Calorimeter (ITC) measurements (Bonnaud et al., 2010). explored the interactions between LAE and different biopolymers

* Corresponding author.
E-mail address: nallamilli@mpip-mainz.mpg.de (T. Nallamilli).

https://doi.org/10.1016/j.crfs.2021.01.003
Received 19 December 2020; Received in revised form 23 January 2021; Accepted 29 January 2021
2665-9271/© 2021 The Author(s). Published by Elsevier B.V. This is an open access article under the CC BY-NC-ND license (http://creativecommons.org/licenses/by-nc-nd/4.0/).

like pectin, carrageenan, xanthan etc. In this study, authors reported that no interactions were observed between LAE and neutral polymer dextran where as strong exothermic interactions were observed between LAE and anionic polysaccharides like pectin, alginate and xanthan (Shtykova et al., 2000; Shtykova et al., 2003). explored the structure of cetylpyridinium chloride and ι-carrageenan using SAXS. In this study, authors reported that pure ι-caraageenan gel did not give any peaks in SAXS while addition of cetyl pyridinium chloride (CPC) showed central scattering and equidistant peaks due to lamellar ordering within the gel (Evmenenko et al., 2001). reported surfactant ordering in cetylpyridinium chloride-κ carrageenan complexes using SANS. In this study, formation of ordered micellar structures formed due to coacervation of Cetylpyridinium chloride and κ-carrageenan were observed using Small Angle Neutron Scattering (SANS) (Loeffler et al., 2014) studied the role of interactions of LAE and anionic polysaccharides on anti-bacterial activity of LAE against spoilage yeasts. In this study authors concluded that interactions between LAE and anionic polysaccharides play a major role in complex formation and also leads to loss in antibacterial activity of LAE.

In this study, we chose a combination of LAE and non-gelling, anionic, algal polysaccharide λ-carrageenan as a model system to understand interactions. λ-carrageenan was chosen as it is widely used in milk products as a viscosity modifier. Also LAE being a simple surfactant like molecule and λ-carrageenan being a charged polyelectrolyte, provides us a model system to understand interactions between such molecules in context of food systems. Several aspects of LAE-λ-carrageenan interactions *viz.* complexation behavior with light scattering, electrophoresis and turbidity measurements have been explored in this study. Using a combination of SAXS and cryo-TEM, the internal structure of complexes is revealed. Thermodynamic interactions of LAE-SDS mixed catanionic micelles with λ-carrageenan were explored using isothermal titration calorimetry. Interfacial behavior of coacervates was also analyzed with tensiometry.

2. Materials and methods

2.1. Materials

Lauric Arginate Ester (MW: 421.02 g/mol) commercially available as MIRENAT-G (10.5% LAE + 89.5% Glycerol) was provided by Vedeqsa Group (Terrassa, Spain). λ-carrageenan (low viscosity, MW. 1,363,000 Da) was purchased from TCI Deutschland GmbH, Germany. Sodium Dodecyl Sulfate (SDS) and Tween 20 (Polyoxyethylene (20) sorbitanmonolaurate) were purchased from Sigma Aldrich (Germany). Distilled and deionized water form a Milli-Q system with conductivity <18.2 MΩ cm was used in all experiments.

2.2. Methods

2.2.1. Sample preparation

All samples of λ-carrageenan were prepared by dissolving pre weighed amounts in deionized water at 60 °C and stirrer speed 400 RPM. Samples were later cooled to 25 °C and stored. LAE solutions were prepared by dissolving pre weighed amounts in deionized water at 25 °C. pH of both LAE and λ-carrageenan were adjusted to 7.0 with dilute hydrochloric acid or sodium hydroxide and mixtures were prepared at desired mixing ratios LAE/carrageenan wt ratio of 0.1, 0.2, 1, 2, 3, 5, 7, 10, 12.5, 15, 17.5, 20.

2.2.2. Turbidity, zeta potential and particle size measurements

Turbidity of samples was measured using a turbidity meter (Eutech-100, Thermo scientific). For each sample turbidity was measured thrice and the mean value of turbidity and corresponding errors were reported. The zeta potential of samples was measured using a Zetasizer nano ZS (Malvern, United Kingdom). Zeta potential for each sample was measured thrice and mean value together with corresponding errors were finally reported. All multiangle light scattering experiments (DLS/SLS) were performed on a commercially available instrument from ALV GmbH (Langen, Germany) consisting of an electronically controlled goniometer and an ALV-5000 multiple tau full-digital correlators with 320 channels (resolution of $10^{-7}s \leq t \leq 10^{3}s$). A HeNe laser with a wavelength of 632.8 nm and an output power of 25 mW (JDS Uniphase, Milpitas, USA, Type 1145P) was utilized as the light source. The samples were diluted to a concentration of 0.1 g/L in water. The solutions were then filtered through Millex LCR filters with a pore size of 0.45 μm (Merck Millipore, Billerica, USA) into dust-free quartz light scattering cuvettes (inner diameter 18 mm, Hellma, Müllheim), which were cleaned before with acetone in a Thurmont-apparatus. The light scattering measurements were then performed at a constant temperature of 20 °C. With dynamic light scattering (DLS) the z-average diffusion coefficients were determined via the CONTIN algorithm after angular dependent measurements and extrapolated to $q = 0$. The hydrodynamic radius was then calculated via the Stokes-Einstein equation. From SLS measurements, the radius of gyration was determined via a Zimm linearization from the slope of the scattering curve.

2.2.3. Small angle X-ray scattering (SAXS)

Small angle X-ray scattering was measured in transmission geometry using Cu K_α, $\lambda = 0.154$ nm radiation (RigakuMicroMax 007 x-ray generator, Osmic Confocal Max-Flux curved multilayer optics). The coacervate sample of 1 mm thickness was contained in a custom cell between two 0.4 mm thick single crystal diamond windows (element six). Scattering data was recorded on an online image plate detector (Mar Research Mar 345) at a sample-detector distance of 352 mm and 2089 mm. Background from cosmic radiation was removed by a rank filter based masking algorithm. The 2D scattering patterns were corrected for standard geometry corrections (Skinner et al., 2012) and radially averaged. The scattering data I(q) vs. $q = 4\pi/\lambda\sin\theta$ was analyzed using Teubner-Strey structure factor model with a phase shift (Teubner and Strey 1987; Weiss et al., 2017). This generic model function describes exponentially decaying, oscillatory function. This model was originally proposed by (Teubner and Strey 1987) to describe density fluctuations in micro emulsions. This model assumes pair correlation function of the form

$$G(r) = \frac{d}{2\pi r}\exp\left(-\frac{r}{\xi}\right)\sin\left(\frac{2\pi r}{d} - \phi\right) \quad (1)$$

Where d is the characteristic domain size or periodicity and ξ is the correlation length, i.e. length beyond which correlations die out and ϕ is phase shift. Samples for SAXS measurements were prepared by adding suitable amounts of LAE to 0.5 wt% solutions of λ-carrageenan. The turbid fractions containing the coacervates were separated by centrifugation at 5000 rpm (3556g) and used for SAXS measurements. Higher concentration of λ-carrageenan was used to obtain larger amount of coacervate as scattering signal obtained from dilute coacervates samples was too weak to be analyzed.

The relative statistical error of the I(q) was found to be smaller than 0.1% for every datapoint and was neglected during the analysis. Standard errors of the detector' dark counts were found to be 0.24 counts per readout per bin. Errors in the fit parameters were estimated using the covariance matrix. The covariance matrix was obtained by multiplying the fractional covariance with the reduced chi, as provided by the SciPy optimize "leastsq" function. Standard deviations were obtained by taking the square root of the diagonal elements of the covariance matrix. For the derived quantity ξ/d, standard deviations of ξ and d were propagated.

2.2.4. Cryo transmission electron microscopy (cryo-TEM)

Samples of liquid coacervate were blotted on to a copper grid (consisting of lacey carbon support mesh) using the FEI Vitrobot (Vitrification Robot) Mark III. Blotted samples were vitrified by manually plunging into liquid ethane and liquid nitrogen (−196 °C). Samples were prepared on

copper grids (200 mesh) with a pattern of 2 μm holes in a carbon support film. The vitrified samples were placed in a cryo-TEM holder and analyzed using a transmission electron microscope (FEI Tecnai F20). Imaging was done at accelerating voltage of 120 kV and temperature of 100 K.

2.2.5. Isothermal titration calorimetry (ITC)

ITC measurements were performed using a Nano ITC Low Volume (TA Instruments, Eschborn, Germany) with an effective cell volume of 170 μL. During each experiment, 50 μL of the respective surfactant solution (LAE/glycol, c_{LAE} = 0.6 wt%/14.34 mM or SDS, c = 0.6 wt %/20.81 mM) were titrated into 300 μL of an aqueous solution of carrageenan (c = 0.01 wt%/7.34·10^{-5}mM). For the titration of carrageenan with mixed surfactants, the total surfactant concentration of LAE + SDS in the syringe was adjusted to 15 mM with fractions of 20%, 50% and 80% SDS. Additionally, the same amount of surfactant solution was titrated into 300 μL of MilliQ water for determining the dilution heat for each experiment. The number of injections was set to 25 for each measurement (25 × 2 μL) with a spacing of 250 s between every injection. For determining the Critical Micelle Concentration (CMC) of LAE, a concentration of c_{LAE} = 1.81 wt%/43.02 mM was chosen and titrated into MilliQ water. The number of injections was set to 50 for each CMC measurement (50 × 1 μL) with a spacing of 250 s between every injection. All measurements were carried out at 25 °C except for the determination of the CMC of LAE at 15 °C. The integrated heats of dilution were subtracted from the integrated heats of every adsorption measurement. The normalized heats were fitted according to an independent binding model (see equation S1 of supporting information) to obtain the association constant (Ka), the reaction enthalpy (ΔH), the entropy (ΔS), the Gibbs free energy (ΔG) and the reaction stoichiometry (n). Each measurement was carried out in triplicate and the mean value as well as standard deviation for each parameter were calculated after baseline correction was made. Data evaluation of the ITC measurements was performed using the Nano Analyze Data Analysis Software (Software version 2.5.0) from TA Instruments.

Analysis of adsorption isotherms from data obtained by ITC experiments was performed using a fit according to an independent binding model (see equation (2)). For this model, it is assumed that a ligand L binds one site of a macromolecule M independently and without any cooperativity effects.

$$q = \left(\frac{(n[M]K_a + [L]K_a + 1) - \sqrt{(n[M]K_a + [L]K_a + 1)^2 - 4NK_a{}^2[M][L]}}{2K_a} \right) - [ML]_{n-1} \mathrm{H} V_{cell} \tag{2}$$

Following equation (2), the stoichiometry n, the association constant K_a and the binding enthalpy ΔH are determined. [M] is given as the concentration of the macromolecule, [L] as the concentration of the ligand, [ML] as the concentration of the formed complex and ΔV_{cell} as the change of the total cell volume during the titration. All values given in the main manuscript are an average of triplicates with the standard deviation of all three experiments. The Gibbs free energy is calculated following the reaction isotherm equation (3), whereas the change in entropy ΔS is calculated by combining equation (3) with the Gibbs-Helmholtz equation (4) and solving for ΔS (equation (5)).

$$G = -RT \ln K_a \tag{3}$$

$$G = H - TS \tag{4}$$

$$S = R \ln K_a + \frac{H}{T} \tag{5}$$

2.2.6. Surface tension measurement

Surface tension of samples was measured using tensiometer (model: DCAT 31 Dataphysics Gmbh, Germany) using a Du nouy ring (model: RG 10) geometry. Samples were prepared with fixed concentration of LAE (2 wt%) and systematically increasing the concentration of the λ-carrageenan from 0 to 1 wt% (0.000, 0.010, 0.025, 0.050,0.075, 0.100, 0.250, 0.300, 0.500, 0.750 and 1.000 wt%). For each sample the measurements were performed thrice and the average value was finally reported. Mean error in each measurement was found to be less than ±0.0016 mN/m.

3. Results and discussion

3.1. Complex coacervation of LAE/λ-carrageenan mixtures

The complexation of LAE and λ-carrageenan was studied by preparing solutions of fixed amount of carrageenan (0.01 wt%) and systematically increasing the amount of LAE (0.001 wt% to 0.200 wt%). As shown in Fig. 1. (a) at very low concentrations of LAE/carrageenan ratio < 0.2 there was no turbidity in the samples indicating no formation of coacervates. When surfactant concentration is below a critical concentration called Critical Aggregation Concentration (CAC) the number of

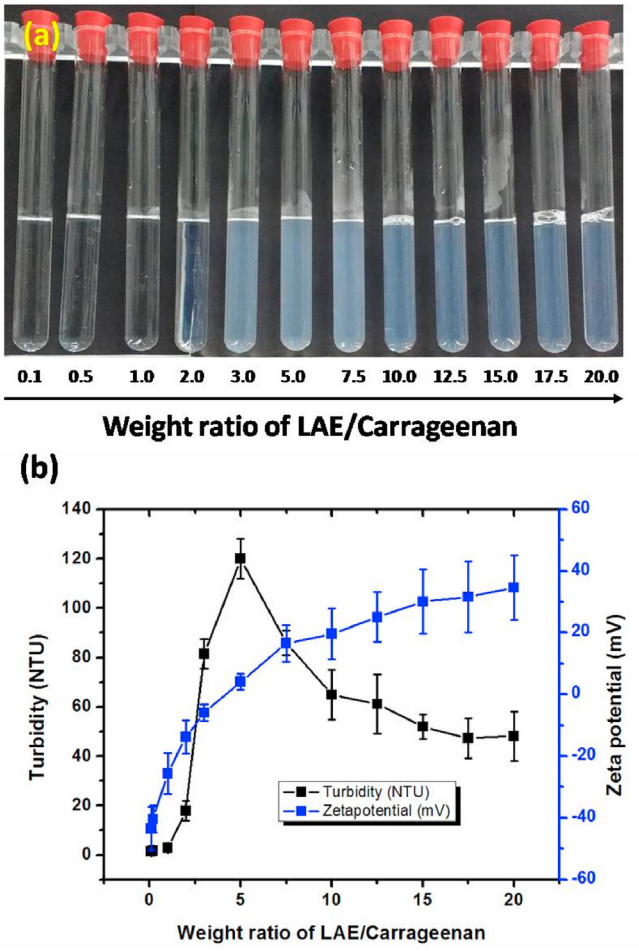

Fig. 1. (a) mixtures of LAE/λ-carrageenan mixtures showing increase in turbidity with increasing weight ratio of LAE/Carrageenan from 0.1 to 20. (b) turbidity (black squares) and zeta potential (blue squares) of samples shown in Fig. 1(a). The concentration of carrageenan in all samples is fixed at 0.01 wt%. (For interpretation of the references to colour in this figure legend, the reader is referred to the Web version of this article.)

surfactant molecules are too few and far separated from each other and the polysaccharide to form any large coacervates. At intermediate LAE/carrageenan ratio 2 to 5 an increase in turbidity was observed in the samples due to formation of complex coacervates. A maximum in turbidity was observed when the LAE to λ-carrageenan weight ratio was 5. Interestingly, with further increase in LAE/carrageenan ratio >5 there was a decrease in turbidity. This is due to overcharging of the complex coacervates (Berret 2005). When excess LAE molecules bind to carrageenan, the large complexes start to redisperse back to form smaller but more positively charged complexes.

Turbidity, zeta potential and particle size of the complexes was monitored along the whole range of LAE/carrageenan ratio. As shown in Fig. 1. (b) a systematic increase in charge, changing from −43.5 mV to +36.6 mV was observed. The maximum in turbidity corresponded to the sample with a zeta potential closest to zero or charge neutrality. The best ratio of LAE/Carrageenan that yields maximum coacervation is 5. Beyond this point zeta potential values increased further to positive values indicating formation of complexes that were positively charged. Particle sizes analysis of complex coacervate samples shown in Fig. 1(a) are presented in Figure SI1, SI2, SI3 and Table SI1 of supporting information. Since coacervation in some samples yielded broad, multimodal size distributions, Hydrodynamic radius (Rh) and Radius of gyration (Rg) could not be determined consistently for all samples.

General phenomenon describing surfactant/polymer complexation was first proposed by (Sata and Saito 1952) in 1954. This simple model is widely known as "Pearls on a string" model (Lam and Walker 2010). As shown in Fig. 2 at very low concentration of surfactant, much below the critical aggregation concentration (CAC) there is no measurable interactions between two species. At CAC there is formation of intermolecular complexes. At surfactant concentration higher than CAC, formation of micelles occurs leading to a complex of surfactant micelles and polymer. This typically leads to formation of large aggregates yielding high turbidity and particle size. In some cases, formation of solid nanoparticles of these complexes is also observed. At surfactant concentration much higher than CAC, the increasing number of charged micelles lead to over-charging of complexes resulting in disintegration of large complexes and formation of smaller but highly charged complexes. Although this hypothesis is well accepted as a general model to describe this phenomenon, in recent years various other architectures of surfactant-polymer complexes have also been reported. The internal structure of complexes can depend on a host of other parameters like stiffness of polymer chain, charge of polymer, architecture of surfactant molecule, ion concentration of solution (Debye length), temperature, etc (Chiappisi et al., 2013).

3.2. Microstructure of complex coacervates

Fig. 3. (a) Shows the SAXS scattering pattern of coacervate solutions for LAE/λ-carrageenan weight ratios 0.86, 1.12, 1.60, 2.22, 3.70, 11.14, 33.42, 77.96, 144.80 and 189.34. In terms of molecular ratios, this corresponds to 0.077, 0.100, 0.143, 0.200, 0.333, 1, 3, 7, 13, 17 LAE molecules per λ-carrageenan monomer, respectively. The 2D scattering image shows a clear isotropic ring, originating from mesoscopic order (inset). For all LAE concentrations, the radial averaged scattering pattern shows a peak at $q_0 \approx 1.61$ nm^{-1}. This suggests that for all ratios there is a preference to form complexes with a mesoscopic order. These ordered structures can be either lamellar or dense packing of micelles within carrageenan sheets. However, if the structure is lamellar with closely packed lamellae with long-range order then higher order peaks should be observed in the scattering pattern (Chang et al., 2018). To confirm the structure of coacervates Cryo-TEM imaging of coacervate samples was performed. Cryo-TEM revealed a lamellar structure as shown in Fig. 4(a). The thickness of each lamella was approximately 4 nm. This confirms that internal structure of coacervates is lamellar and not micellar aggregates.

Based on the position of the peak value of scattering vector ($q_0 = 1.6$ nm^{-1}), a periodicity value of $d = 2\pi/q_0 \sim 3.9$ nm was calculated. With a diameter of 0.6 nm for the carrageen chain, 0.9 nm for the positively charged surfactant head group, and 1.4 nm for the LAE C_{11} alkyl chain we estimate a maximum periodicity of 3.8 nm and 5.2 nm for a bilayer with interdigitated and extended chains, respectively. Therefore, the periodicity of 3.9 nm observed in SAXS is consistent with the formation of a lamellar structure composed of LAE bilayers sandwiched between carrageen sheets. Similar bilayer like structures were reported for ι-carrageenan/ionic surfactant solution (Shtykova et al., 2000). Lamellar periodic structures form by complex coacervation of λ-carrageenan and an ionic surfactant LAE. The driving force for the coacervation are hydrophobic and electrostatic interactions of the LAE and λ-carrageenan.

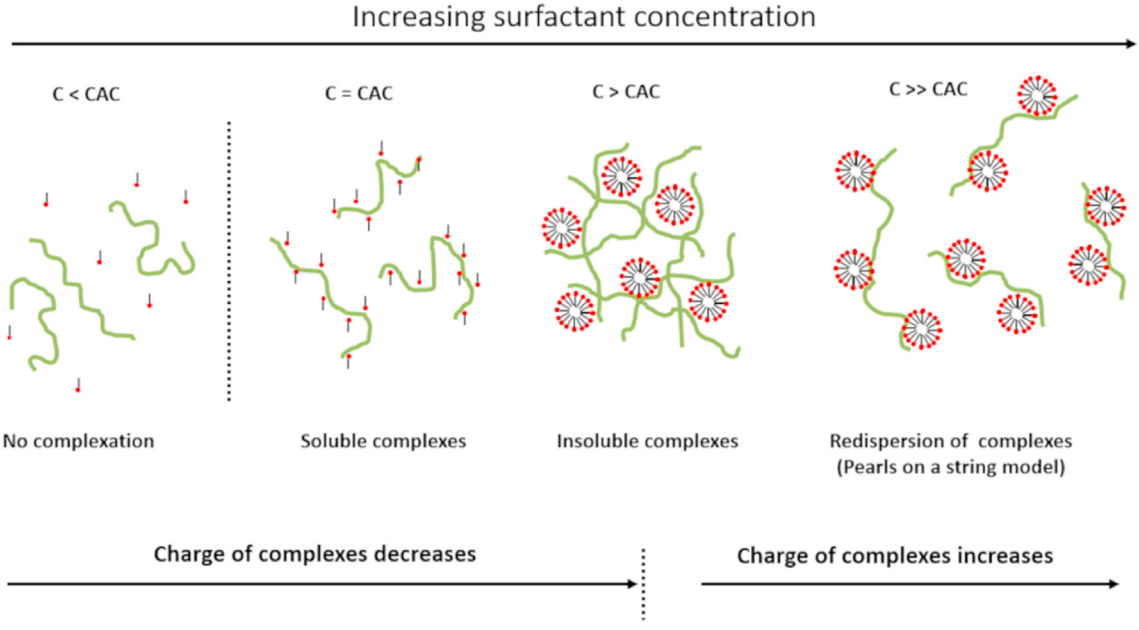

Fig. 2. Schematic illustration of "pearls on a string" model of surfactant-polymer complexation. At surfactant concentration C < CAC no complexation happens, at C = CAC formation of soluble complexes occurs, at C > CAC formation of large insoluble complexes occurs with development of high turbidity and finally C » CAC complexes contain excess surfactant leading to over-charging of complexes and eventually leading to redispersion of complexes and reduction in turbidity.

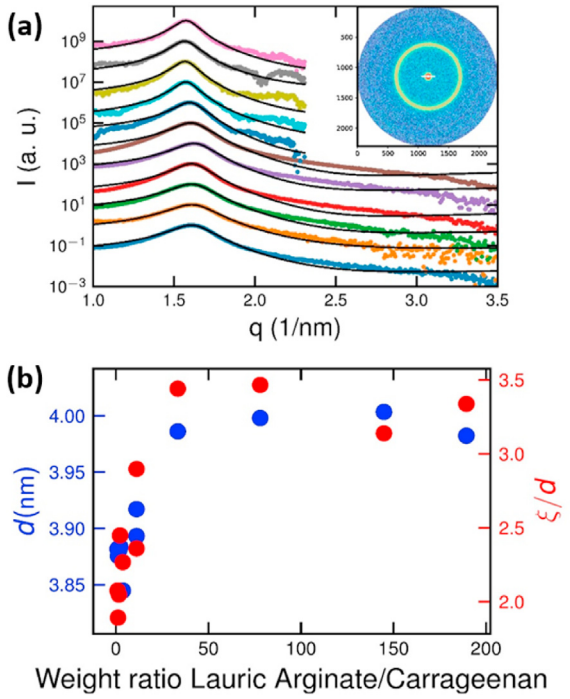

Fig. 3. (a) Scattering pattern of LAE/λ-carrageenan solutions (inset) and radial averages for LAE/λ-carrageenan weight ratios of 0.86 (blue bottom curve) to 189.34 (pink top curve). For all concentrations, a scattering peak is found at $q_0 \approx 1.6\ nm^{-1}$. (b) Periodicity d (blue) and normalized correlation length ξ/d (red) for different LAE/λ-carrageenan ratios obtained by fitting a Teubner-Strey structure factor to the SAXS peak. The λ-carrageenan concentration in all samples is fixed at 0.5 wt%. (For interpretation of the references to colour in this figure legend, the reader is referred to the Web version of this article.)

The negatively charged backbone of λ-carrageenan locally helps the LAE molecules to order themselves into bilayers. In the space between two bilayers, the water molecules reside and the hydrophilic λ-carrageenan molecules arrange themselves in between the bilayers.

Quantitative analysis by fitting a Teubner-Strey structure factor yields a periodicity of the lamellae of $3.75 < d < 4.01$ nm (Fig. 3 (b), blue circles). For LAE/λ-carrageenan ratios ≤33.42 the periodicity d increases with increasing LAE ratio. This indicates a higher packing density of LAE with increasing concentration. However, for LAE ratios >33.42, the periodicity d saturates at d ≈ 4 nm. Simultaneously, the normalized correlation length ξ/d increases from 1.9 to 3.5 (Fig. 3 (b), red circles). As found for the periodicity d, constant values of $\xi/d \approx 3.2$ are found above LAE ratios of 33.42. For the positively charged LAE fully occupying the negatively charged sites on λ-carrageenan, electrostatic repulsion of the carrageenan chain segments is reduced. When the LAE/carrageenan ratio is low, the LAE molecules have more space between themselves and thus a large fraction of them will be in tilted configuration (due to high entropy) leading to less spacing between the carrageenan layers. As the LAE/Carrageenan ratio increases the LAE molecules get more densely packed and adopt straight configuration, perpendicular to carrageenan layers, leading to bilayer thickness almost close to 4 nm, which is approximately twice the length of LAE molecule.

For a smectic mesophase with long-range order, we would expect Bragg like scattering peaks with higher order reflections. However, in the SAXS measurements only a single broad peak is observed. This indicates that the lamellar order of the LAE molecules and carrageen chains is only short-ranged. This can be explained by comparing the cross section of LAE molecules with the area density of charged sites available on the carrageenan backbone. From its molecular structure and a bulk density of 1.72 gm/cm^3 for carrageenan we estimate an area of 38 Å^2 per negative charge within the carrageen sheets (details in Supporting Information). In natural carrageen, this value might be even higher due to the occasional presence of uncharged regions in the carrageenan backbone. Thus, the density of charged sites is about twice the cross section of approximately 20 Å^2 found for closed packed alkyl chains in surfactants or surface phases (Ocko et al., 1997). Therefore, the extra space available allows for tilts and gauge defects in the LAE alkyl chains. This induces fluctuations in the spacing between subsequent carrageenan sheets leading to disorder of the lamellar arrangement as shown in Fig. 4(a) and (b). Hence, it may be concluded that the broad scattering peak without higher order peaks for LAE/λ-carrageenan complexes results from a lamellar structure composed of LAE bilayers in-between carrageenan sheets. Within the bilayers, the LAE molecules are not perfectly close packed but arranged with some degree of disorder and lamellae do not have a long-range order.

3.3. Effect of micelle charge on complex formation

Most of the cationic molecule like Lauric Arginate Ester (LAE) have bitter taste (Asker et al., 2011) and their strong interactions with anionic polysaccharides in food products increases their amount to be added to achieve desired degree of efficiency. In this study, we explore the interaction of mixed micelles of LAE/Tween 20 (cationic + nonionic) and LAE/SDS (cationic + anionic) surfactants with λ-carrageenan.

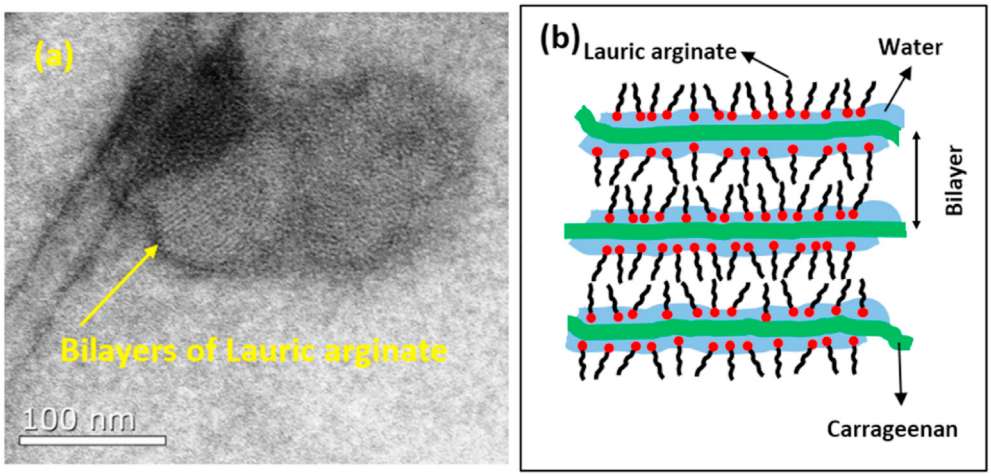

Fig. 4. (a) Cryo-TEM image of LAE/λ-carrageenan complex coacervate particles. The coacervate particle size is about 250 nm. Inset shows the schematic representation of internal structure of coacervates. Weight ratio of LAE/λ-carrageenan in this sample is 33.42:1. Concentration of λ-carrageenan is 0.5 wt% (b) Schematic illustration of internal structure of coacervate showing bilayers in which LAE molecules are arranged with certain degree of disorder.

3.3.1. LAE-Tween 20 (cationic-nonionic mixed micelles)

Mixed micelle solutions were prepared by mixing solutions of LAE (0.15 wt%) and Tween 20 (0.00, 0.02, 0.03, 0.05, 0.07, 0.10, 0.15, 0.20, 0.30, 0.40, 0.50, 0.60 wt%) at different ratios. These mixed micelle solutions were added to λ-carrageenan solutions (0.02 wt%) to observe the effect of micelle charge on complex formation. As shown in Fig. 5. (a) and 5. (b) there was a decrease in turbidity of the samples from 227 NTU with mixture of pure LAE and λ-carrageenan to 43.1 NTU with (LAE + Tween 20). The decrease in turbidity indicates that the size of the complexes formed is decreasing due to decreased interactions between mixed micelles and carrageenan. Due to increased fractions of Tween 20 in the micelles, the charge of micelles will be less positive thus reducing the interaction strength and consequently leading to smaller complex particles. There was also a slight increase in the zeta potential values of samples from +9.65 mV (pure LAE + carrageenan) to +13.33 mV (LAE + Tween 20/carrageenan). This may be due to two possible reasons, first reason being that increasing amounts of Tween 20 in the samples lead to formation of a higher number of mixed micelles, which are positively charged. Additionally, as concentration of Tween 20 increases the number of mixed micelles will be in a greater number, with greater over all surface area which strongly contribute to the electrophoretic mobility/scattered light, which eventually reflects in measured zeta potential values. Similar reduction in interactions between mixed micelles of LAE/Tween20 and pectin were reported by (Asker et al., 2011).

3.3.2. LAE-SDS (cationic-anionic mixed micelles)

When oppositely charged surfactants are mixed, it leads to the formation of catanionic micelles or vesicles (Chakraborty and Sarkar 2004; Tah et al., 2011). Fig. 6. (a) Shows mixtures of LAE and SDS mixed at different mixing fractions ranging from 0 to 1 with 0.1 intervals prepared using 0.631 wt% LAE and 0.432 wt% SDS. It is observed that at extreme compositions, the solutions are clear indicating only micelle formation. Micelles being very small (<10 nm) do not scatter much light and thus give clear solutions. However, at intermediate compositions there is an increase in turbidity indicating formation of large catanionic vesicles. Since these vesicles consist of both positive and negative surfactant molecules, their overall charge is less compared to individual micelles of pure surfactants. Size distribution of samples shown in Fig. 6 (a) were analyzed using multi angle light scattering and are given in Figure SI4, SI5, SI6 and Table SI2 of supporting information.

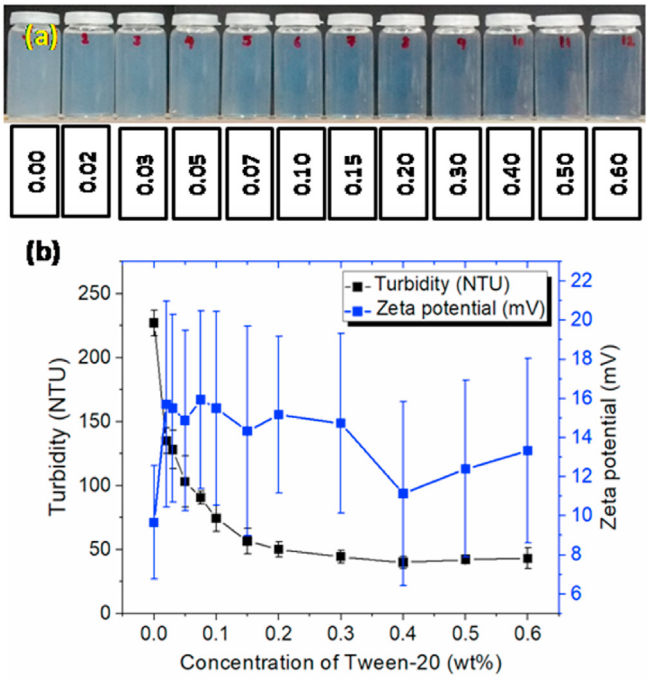

Fig. 5. (a) Turbidity of the samples in which mixed micelle solutions of LAE/Tween 20 were mixed with λ-carrageenan solutions. Wt% of LAE was fixed 0.15 wt% and wt% of Tween-20 in mixed micelles is increased as shown. (b) Zeta potential and turbidity of samples shown in Fig. 5(a). As zeta potentials were low (˂ 25 mV) the error in repeated measurements was found to be large. Concentration of λ-carrageenan is 0.02 wt% in all samples. Concentration of LAE is 0.15 wt%.

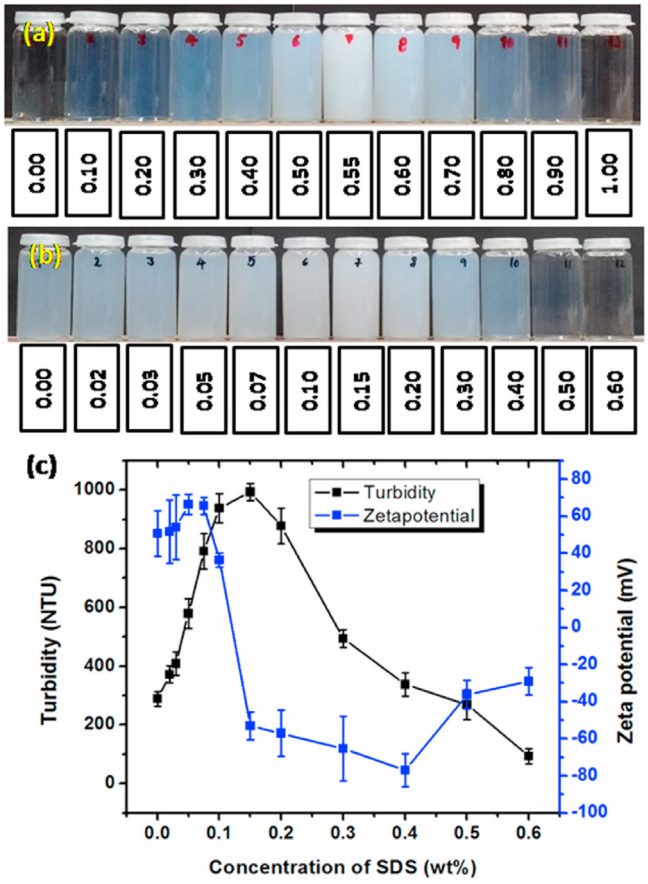

Fig. 6. (a)Mixtures of pure LAE and SDS mixed at different SDS mole fractions from 0 to 1 at 0.1 intervals prepared using 0.631 wt% LAE and 0.432 wt% SDS, weight fraction of SDS is shown. **(b)** Turbidity of samples formed by mixing (LAE + SDS) mixed micelles into 0.02 wt% λ-carrageenan solutions. wt% of LAE was fixed 0.15 wt% and wt% of SDS in mixed micelles is increased as shown. **(c)** Zeta potential (blue) and turbidity (black) of samples shown in Fig. 6(b). Concentration of λ-carrageenan is 0.02 wt% in all samples. Concentration of LAE is 0.15 wt%. (For interpretation of the references to colour in this figure legend, the reader is referred to the Web version of this article.)

Mixed micelle solutions were prepared by mixing LAE (0.15 wt%) and SDS (0.02, 0.03, 0.05, 0.07, 0.10, 0.15, 0.20, 0.30, 0.40, 0.50 and 0.60 wt %). These mixed micelle solutions were added to λ-carrageenan solutions (0.02 wt%) at different LAE/SDS ratios. As shown in Fig. 6. (b) there was a slight increase in turbidity followed by complete disappearance of turbidity at high SDS/LAE weight ratios above 3.33. This is a very interesting result as the formation of complexes is completely suppressed by the presence of SDS. Fig. 6. (c) Shows zeta potential measurements demonstrating that at low SDS/LAE ratio the micelles/vesicles are predominantly positively charged, which allows formation of complexes with negatively charged carrageenan. As the SDS/LAE ratio increases, the vesicles start to become predominantly negatively charged, which hinders the electrostatic attraction between negatively charged mixed micelles and carrageenan. There is also reduction in turbidity as at high SDS/LAE ratios the mixed micelles are formed, which mainly consist of SDS molecules and thus do not scatter light as much as larger vesicles. The extent to which this interaction occurs depends on the SDS/LAE

ratio. Unlike LAE-Tween 20 mixtures where complex formation can be observed even at high Tween20/LAE ratios, the SDS-LAE system shows a complete lack of complex formation. Fig. 7 Shows the schematic representation of a proposed mechanism.

To get better physical insight into the observations made with LAE/SDS mixed micelle-λ-carrageenan interactions, further measurements were performed with isothermal titration calorimetry (ITC), results of which are discussed in following section.

3.4. Isothermal titration calorimetry

Thermodynamic interactions of LAE and SDS with λ-carrageenan were analyzed with isothermal titration calorimetry. First, the CMC of LAE was determined by titrating an aqueous solution of 1.8 wt% (42.40 mM) LAE into MilliQ water at 15 °C. The resulting thermogramis shown in Figure. SI7of the supporting information. The integrated heats obtained from the corrected heat rate were fitted according to an independent site binding model, where the inflection point yields the CMC. In this case, the inflection point occurred at approximately 5.2 ± 0.1 mM, which corresponds to the CMC of LAE. The value obtained is in good agreement with the value of 4.9 ± 0.2 reported previously by (Asker et al., 2008).

To evaluate interactions between LAE, SDS and λ-carrageenan, thermogramswere obtained at 25 °C by injecting pure aqueous LAE and pure aqueous SDS solutions separately into aqueous λ-carrageenan solutions. Additionally, the heat of dilution for each experiment was determined by titrating the same LAE or SDS solution into pure water and afterwards subtracted from the titration heats. LAE/SDS concentrations were adjusted to be below the respective CMC in the measurement cell during the whole titration process. The obtained corrected heat rates together with the adsorption isotherms are displayed in Fig. 8.

As shown in Fig. 8. (a) Exothermic peaks were observed when LAE was titrated to λ-carrageenan. This is due to strong attractive electrostatic interactions between the oppositely charged LAE and λ-carrageenan. Since SDS and λ-carrageenan are both negatively charged, a smaller heat evolution during their interaction was observed. The integrated adsorption isotherms were fitted according to an independent binding model to extract thermodynamic parameters. Table 1. Shows the association constant K_a, binding enthalpy ΔH, change of entropy ΔS, change of Gibbs free energy ΔG and stoichiometry n of LAE-carrageenan and SDS-carrageenan interactions.

In case of LAE/λ-carrageenan, the association constant (binding affinity) was higher than that for SDS, which means that a stronger interaction occurred. Also, for LAE ($\Delta H_{LAE} = -5.5 \pm 0.1$ kJ mol^{-1}) the enthalpy change was larger and almost twice that of SDS ($\Delta H_{SDS} = -2.6 \pm 0.3$ kJ mol^{-1}) as indicated by the heat flow rates. However, in both

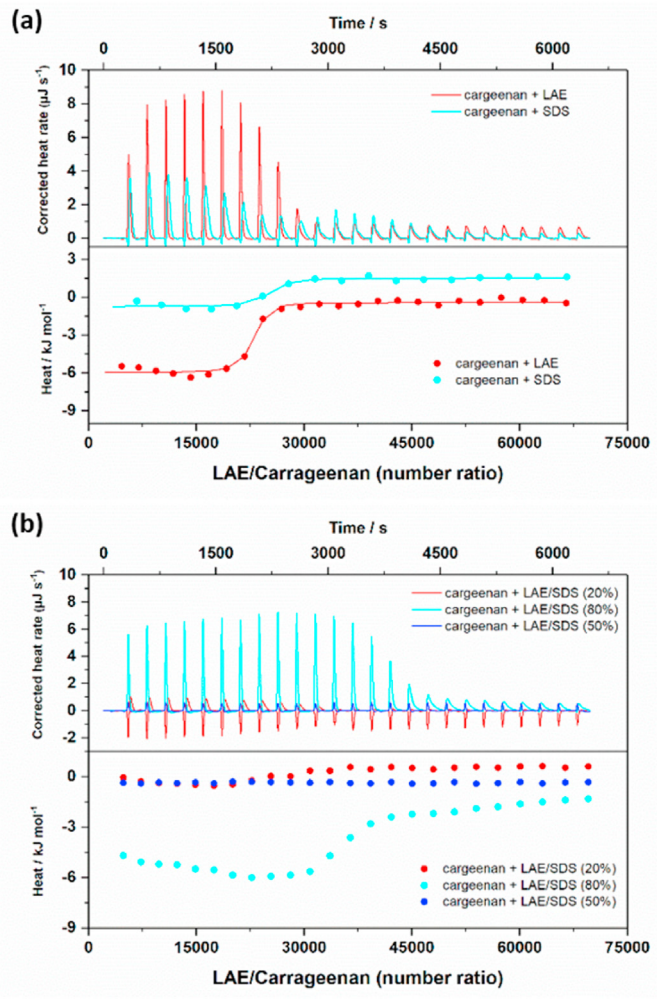

Fig. 8. (a) Corrected heat rates (upper graphs) and corresponding adsorption isotherms (lower graphs) of a) obtained by titrating pure LAE or SDS solutions in to carrageenan solutions. Isotherms for pure surfactant solutions were fitted according to an independent binding model (solid lines). (b) Thermograms obtained by titrating mixed micelle solutions of LAE/SDS in different molar ratios to λ-carrageenan solutions at 25 °C.

cases there was a significant contribution from an entropy gain (at T = 298 K, $T\Delta S_{LAE} = 27.118$ kJ mol^{-1}, $T\Delta S_{SDS} = 28.906$ kJ mol^{-1}) which can be concluded to be the main driving force for the interaction. This can be due to two main contributions: Firstly hydrophobic interactions between

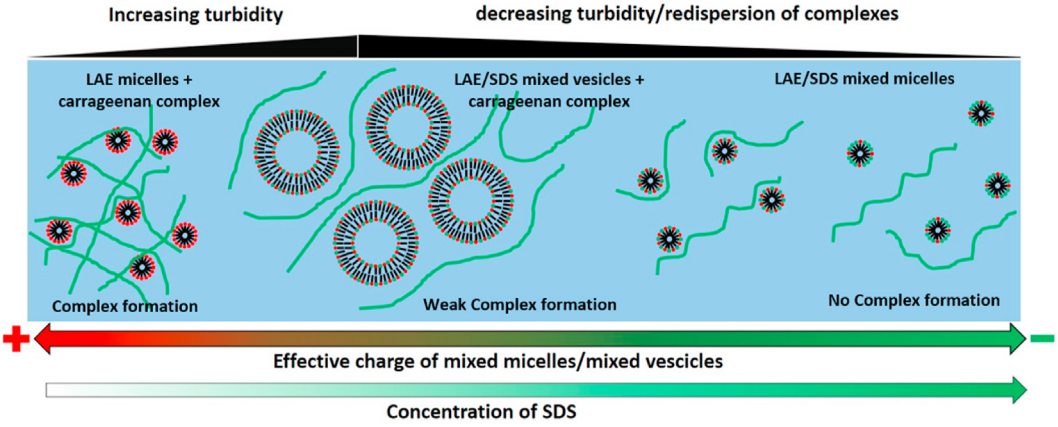

Fig. 7. Schematic representation of a proposed mechanism of interaction between LAE/SDS mixed micelles/vesicles and λ-carrageenan with increasing SDS/LAE ratios.

Table 1
Thermodynamic parameters obtained by fitting an independent binding model to data from isotherms (25 °C) shown in Fig. 8(a).

	LAE + λ-Carrageenan	SDS + λ-Carrageenan
Association constant $K_a/10^6$ M^{-1}	0.51 ± 0.05	0.35 ± 0.10
Enthalpy ΔH/kJ mol^{-1}	−5.5 ± 0.1	−2.6 ± 0.3
Entropy ΔS/J mol^{-1} K^{-1}	91 ± 1	97 ± 2
Gibbs free energy ΔG/kJ mol^{-1}	−33 ± 1	−31 ± 1
Stoichiometry, n	23000 ± 3800	22400 ± 2200

λ-carrageenan and the hydrophobic tails of the surfactants and secondly counter ion release and restructuring of water molecules around formed complexes. Due hydrophobic interactions, water molecules are released from the hydration shells of both LAE, SDS and λ-carrageenan molecules into the bulk water phase, thus leading to an increase in total entropy of the system. The Gibbs free energy of both cases was almost similar in magnitude, indicating that the overall interaction of LAE with carrageenan is only slightly preferred over the interaction of SDS with carrageenan. This probably originates from the additional attractive electrostatic interaction in that system. The interaction stoichiometry in case of LAE was 23000 ± 3800 LAE molecules per λ-carrageenan molecule and 22400 ± 2200 for SDS, which again is not significantly different.

Further, to understand the interaction of mixed catanionic micelles of LAE/SDS with λ-carrageenan, mixed micelle solutions of LAE/SDS with molar ratios of 20/80, 50/50 and 80/20 were titrated into λ-carrageenan solutions to observe the interaction of mixed micelles with λ-carrageenan. As shown in Fig. 8. (b) 80/20 LAE/SDS mixture showed an exothermic interaction with λ-carrageenan almost similar to the pure LAE/λ-carrageenan interaction as in Fig. 8. (a). The 50/50 LAE/SDS solution showed significantly less exothermic signals indicating that almost no interaction takes place. The 20/80 LAE/SDS solution interestingly showed slightly stronger interaction than 50/50 LAE/SDS but significantly lower than 80/20 LAE/SDS. As mixed micelles/vesicles consist of both LAE and SDS molecules fitting of independent binding model to extract thermodynamic parameters and stoichiometry may not be very meaningful. However, heat flow curves conclusively indicate that interactions become weaker as the fraction of SDS molecules increases up to 50% and become slightly stronger again at 80% SDS. ITC measurements also supports our hypothesis that mixed catanionic micelles/vesicles interact to a very limited extent compared to pure surfactants micelles. These results suggest that the presence of an anionic surfactant can significantly reduce the interactions between a cationic surfactant and polymer. This method of mixing LAE with anionic surfactant may be useful in reducing its interactions with anionic polysaccharides, which are often used in food products as thickeners and rheology modifiers and thus may help in improving its anti-microbial properties even with minimal dosages.

3.5. Interfacial and foaming properties

LAE being an amphiphilic molecule shows good emulsifying and foaming tendency. In a recent study (Ma et al., 2016) have shown that mixtures of lecithin and LAE have good emulsifying properties. To observe the interfacial and foaming behavior of LAE/λ-carrageenan complexes, samples were prepared with fixed concentration of LAE (2 wt %) and systematically increasing the concentration of the λ-carrageenan from 0 to 1 wt%. As shown in Fig. 9. (a) complex formation was observed with increasing concentration of λ-carrageenan. When these solutions were foamed by shaking the samples with hand for 30 s and allowed to settle, a decreasing trend in foam volume was observed as shown in Fig. 9. (b). A possible reason for a reduction in foam volume in LAE-carrageen mixtures is that due to complex formation all the LAE molecules are bound in the complexes, which reduces the available LAE molecules for surface activity/foam stabilization. Moreover, the hydrophobic tails of the LAE molecules are directed inward due to formation of bilayers as discussed in the previous section 3.2 on microstructure. This will leave the polar head groups/hydrophilic parts of the LAE molecules and the λ-carrageenan, which is also hydrophilic, exposed towards the surfaces of the complex particles. Thus, effectively the complex coacervate particles behave like hydrophilic particles, which prefer to remain in water phase thus showing very low or no surface activity leading to reduction in foam volume.

Surface tension of LAE/λ-carrageenan mixtures were measured using a tensiometer. As shown in Fig. 10 with increasing concentration of λ-carrageenan there was an increase in the surface tension from about 24.08 ± 0.0016 mN/m to 36.92 ± 0.0016 mN/m. This clearly suggests that with increasing λ-carrageenan concentration the LAE molecules available for surface activity are reduced, which in turn leads to increase in surface tension. Samples above 0.3 wt% of carrageenan were too viscous for obtaining consistent measurements of surface tension.

4. Conclusions

The coacervation behavior of Lauric arginate ester (LAE) with λ-carrageenan was studied in this work. Formation of coacervates was observed in the LAE/carrageenan weight ratio of 2 and maximum coacervation at a ratio of 5. With further increase in ratio, redispersion of coacervates was observed. The microstructure of these coacervates was found to consist of bilayer arrangements of loosely packed LAE molecules with a degree of disorder giving a broad peak in the SAXS scattering pattern with out higher order scattering peaks. Thermodynamic interactions of pure LAE and SDS with λ-carrageenan were predominantly due to entropic contribution arising from hydrophobic interactions, counter ion release and reorganization of water molecules associated with λ-carrageenan. LAE/Tween20 mixed micelles showed a reduction in

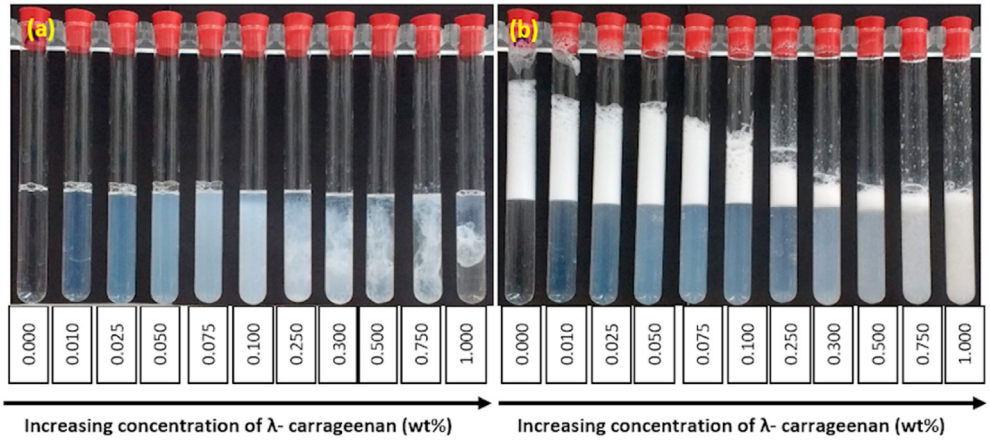

Fig. 9. (a) Mixtures of fixed concentration of LAE (2 wt%) with increasing concentration of λ-carrageenan. **(b)** Freshly foamed samples (same samples in Fig. 9(a)) showing reduction in foam volume as concentration of λ-carrageenan is increased.

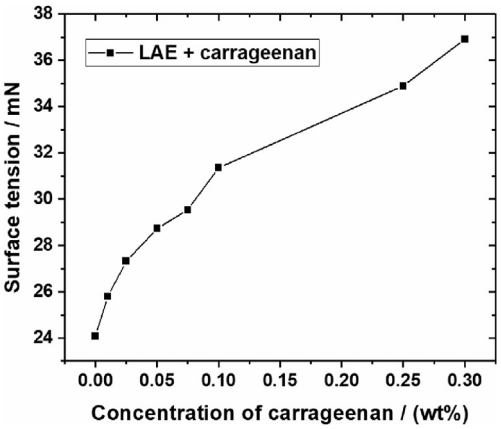

Fig. 10. Surface tension of LAE/λ-carrageenan mixtures (shown in Fig. 9(a)) measured using a tensiometer with Du noüy ring geometry. An increase in surface tension was observed with increase in carrageenan concentration.

turbidity due to a reduction in the overall charge of the micelles. LAE/SDS mixed micelles showed interactions based on the ratio of SDS/LAE. The enthalpy of interaction was highest for low SDS/LAE ratios and decreased as the SDS/LAE ratio increased to 1. These results suggest that the presence of an anionic surfactant can significantly reduce the interactions between a cationic surfactant and polymer. While pure LAE showed good foaming property, its complexes with λ-carrageenan showed very poor foaming properties. This was due to the LAE/carrageenan complexes being hydrophilic, tending to remain in water phase and showing no surface activity leading to reduction in foam volume.

Polymer theory group

Max Planck Institute for polymer research, Ackermannweg-10, Mainz 55128, Germany.

CRediT authorship contribution statement

Trivikram Nallamilli: Conceptualization, Writing original draft, investigation, formal analysis, Validation. **Markus Ketomaeki:** investigation, formal analysis, Validation, **Domenik Prozeller:** investigation, formal analysis, Validation, review and editing. **Julian Mars:** investigation, formal analysis, Validation, review and editing. **Svenja Morsbach:** investigation, formal analysis, Validation, review and editing. **Markus Mezger:** Conceptualization, review and editing. **Thomas Vilgis:** Conceptualization, review and editing.

CRediT authorship contribution statement

Trivikram Nallamilli: Conceptualization, Writing original draft, Investigation, Formal analysis, Validation. **Markus Ketomaeki:** Investigation, Formal analysis, Validation. **Domenik Prozeller:** Investigation, Formal analysis, Validation, review and editing. **Julian Mars:** Investigation, Formal analysis, Validation, review and editing. **Svenja Morsbach:** Investigation, Formal analysis, Validation, review and editing. **Markus Mezger:** Conceptualization, review and editing. **Thomas Vilgis:** Conceptualization, review and editing.

Declaration of competing interest

The authors declare that they have no known competing financialinterestsor personal relationships that could have appeared to influence the work reported in this paper.

Acknowledgements

Trivikram Nallamilli gratefully acknowledges the support of Alexander von Humboldt foundation for postdoctoral fellowship. We gratefully thank Vedeqsa Group (Terrassa, Spain) for providing the samples of Lauric Arginate (Mirenat - G) for this study. We thank Dr. Ingo Lieberwirth for his assistance in TEM imaging of the coacervate samples. We thank Elke Muth for her assistance in surface tension measurements and Christine Rosenauer for her assistance in particle size measurements with multi angle light scattering.

Appendix A. Supplementary data

Supplementary data to this article can be found online at https://doi.org/10.1016/j.crfs.2021.01.003.

References

Asker, D., Weiss, J., McClements, D., 2008. Analysis of the interactions of a cationic surfactant (lauric arginate) with an anionic biopolymer (pectin): isothermal titration calorimetry, light scattering, and microelectrophoresis. Langmuir 25 (1), 116–122.
Asker, D., Weiss, J., McClements, D., 2011. Formation and stabilization of antimicrobial delivery systems based on electrostatic complexes of cationic– non-ionic mixed micelles and anionic polysaccharides. J. Agric. Food Chem. 59 (3), 1041–1049.
Berret, J., 2005. Evidence of overcharging in the complexation between oppositely charged polymers and surfactants. J. Chem. Phys. 123 (16), 164703.
Bonnaud, M., Weiss, J., McClements, D.J., 2010. Interaction of a food-grade cationic surfactant (lauric arginate) with food-grade biopolymers (pectin, carrageenan, xanthan, alginate, dextran, and chitosan). J. Agric. Food Chem. 58 (17), 9770–9777.
Chakraborty, H., Sarkar, M., 2004. Optical spectroscopic and TEM studies of catanionic micelles of CTAB/SDS and their interaction with a NSAID. Langmuir 20 (9), 3551–3558.
Chang, C.-W., Cheng, M.-H., Ko, H.-W., Chu, C.-W., Tu, Y.-H., Chen, J.-T.J. S. m., 2018. Microwave-annealing-induced nanowetting of block copolymers in cylindrical nanopores, 14 (1), 35–41.
Chiappisi, L., Hoffmann, I., Gradzielski, M., 2013. Complexes of oppositely charged polyelectrolytes and surfactants–recent developments in the field of biologically derived polyelectrolytes. Soft Matter 9 (15), 3896–3909.
Covis, R., Vives, T., Gaillard, C., Benoit, M., Benvegnu, T., 2015. Interactions and hybrid complex formation of anionic algal polysaccharides with a cationic glycine betaine-derived surfactant. Carbohydr. Polym. 121, 436–448.
Dai, Y., Normand, M.D., Weiss, J., Peleg, M., 2010. Modeling the efficacy of triplet antimicrobial combinations: yeast suppression by lauric arginate, cinnamic acid, and sodium benzoate or potassium sorbate as a case study. J. Food Protect. 73 (3), 515–523.
De Kruif, C.G., Weinbreck, F., de Vries, R., 2004. Complex coacervation of proteins and anionic polysaccharides. Curr. Opin. Colloid Interface Sci. 9 (5), 340–349.
Evmenenko, G., Theunissen, E., Mortensen, K., Reynaers, H., 2001. SANS study of surfactant ordering in κ-carrageenan/cetylpyridinium chloride complexes. Polymer 42 (7), 2907–2913.
Hu, X., Huang, E., Barringer, S.A., Yousef, A.E., 2020. Factors affecting Alicyclobacillus acidoterrestris growth and guaiacol production and controlling apple juice spoilage by lauric arginate and ε-polylysine. LWT 119, 108883.
Jun-xia, X., Hai-yan, Y., Jian, Y., 2011. Microencapsulation of sweet orange oil by complex coacervation with soybean protein isolate/gum Arabic. Food Chem. 125 (4), 1267–1272.
Kayitmazer, A.B., 2017. Thermodynamics of complex coacervation. Adv. Colloid Interface Sci. 239, 169–177.
Kevelam, J., van Breemen, J.F., Blokzijl, W., Engberts, J.B., 1996. Polymer– surfactant interactions studied by titration microcalorimetry: influence of polymer hydrophobicity, electrostatic forces, and surfactant aggregational state. Langmuir 12 (20), 4709–4717.
Lam, V.D., Walker, L.M., 2010. A pH-induced transition of Surfactant– polyelectrolyte aggregates from cylindrical to string-of-pearls structure. Langmuir 26 (13), 10489–10496.
Lau, I.P., Chen, H., Wang, J., Ong, H.C., Leung, K.C.-F., Ho, H.P., Kong, S.K.J.N., 2012. In vitro effect of CTAB-and PEG-coated gold nanorods on the induction of eryptosis/erythroptosis in human erythrocytes, 6 (8), 847–856.
Loeffler, M., McClements, D., McLandsborough, L., Terjung, N., Chang, Y., Weiss, J., 2014. Electrostatic interactions of cationic lauric arginate with anionic polysaccharides affect antimicrobial activity against spoilage yeasts. J. Appl. Microbiol. 117 (1), 28–39.
Ma, Q., Davidson, P.M., Zhong, Q.J. F.c., 2016. Nanoemulsions of Thymol and Eugenol Co-emulsified by Lauric Arginate and Lecithin, vol. 206, pp. 167–173.
Ma, Q., Davidson, P.M., Zhong, Q., 2020. Properties and potential food applications of Lauric arginate as a cationic antimicrobial. Int. J. Food Microbiol. 315, 108417.
Martins, I.M., Barreiro, M.F., Coelho, M., Rodrigues, A.E., 2014. Microencapsulation of essential oils with biodegradable polymeric carriers for cosmetic applications. Chem. Eng. J. 245, 191–200.

Miquelim, J.N., Lannes, S.C., Mezzenga, R., 2010. pH Influence on the stability of foams with protein–polysaccharide complexes at their interfaces. Food Hydrocolloids 24 (4), 398–405.
Ocko, B., Wu, X., Sirota, E., Sinha, S., Gang, O., Deutsch, M., 1997. Surface freezing in chain molecules: normal alkanes. Phys. Rev. 55 (3), 3164.
Okuzaki, H., Osada, Y., 1994. Effects of hydrophobic interaction on the cooperative binding of a surfactant to a polymer network. Macromolecules 27 (2), 502–506.
Saravanan, M., Rao, K.P., 2010. Pectin–gelatin and alginate–gelatin complex coacervation for controlled drug delivery: influence of anionic polysaccharides and drugs being encapsulated on physicochemical properties of microcapsules. Carbohydr. Polym. 80 (3), 808–816.
Sata, N., Saito, S., 1952. Die solubilisation von Polyvinylazetat. Colloid Polym. Sci. 128 (3), 154–158.
Shtykova, E., Dembo, A., Makhaeva, E., Khokhlov, A., Evmenenko, G., Reynaers, H., 2000. SAXS study of ι-carrageenan− surfactant complexes. Langmuir 16 (12), 5284–5288.
Shtykova, E.V., Shtykova Jr., E.V., Volkov, V.V., Konarev, P.V., Dembo, A.T., Makhaeva, E.E., Ronova, I.A., Khokhlov, A.R., Reynaers, H., Svergun, D.I., 2003. Small-angle X-ray scattering reveals hollow nanostructures in-and-carrageenan/surfactant complexes. J. Appl. Crystallogr. 36 (3), 669–673.
Skinner, L.B., Benmore, C.J., Parise, J.B., 2012. Area detector corrections for high quality synchrotron X-ray structure factor measurements. Nucl. Instrum. Methods Phys. Res. Sect. A Accel. Spectrom. Detect. Assoc. Equip. 662 (1), 61–70.
Stewart, R.J., Wang, C.S., Shao, H., 2011. Complex coacervates as a foundation for synthetic underwater adhesives. Adv. Colloid Interface Sci. 167 (1–2), 85–93.
Tah, B., Pal, P., Mahato, M., Talapatra, G., 2011. Aggregation behavior of SDS/CTAB catanionic surfactant mixture in aqueous solution and at the air/water interface. J. Phys. Chem. B 115 (26), 8493–8499.
Teubner, M., Strey, R., 1987. Origin of the scattering peak in microemulsions. J. Chem. Phys. 87 (5), 3195–3200.
Waite, J.H., Andersen, N.H., Jewhurst, S., Sun, C., 2005. Mussel adhesion: finding the tricks worth mimicking. J. Adhes. 81 (3–4), 297–317.
Weiss, H., Mars, J., Li, H., Kircher, G., Ivanova, O., Feoktystov, A., Soltwedel, O., Bier, M., Mezger, M., 2017. Mesoscopic correlation functions in heterogeneous ionic liquids. J. Phys. Chem. B 121 (3), 620–629.
Wu, B.-c., Degner, B., McClements, D.J., 2014. Soft matter strategies for controlling food texture: formation of hydrogel particles by biopolymer complex coacervation. J. Phys. Condens. Matter 26 (46), 464104.